Electric Power Systems Research 154 (2018) 515–527

Contents lists available at ScienceDirect

Electric Power Systems Research

journal homepage: www.elsevier.com/locate/epsr

Sensitivity analysis of method for harmonic state estimation in the power system

Vedad Bečirović [a,*], Ivica Pavić [b], Božidar Filipović-Grčić [b]

[a] Faculty of Electrical Engineering, University of Sarajevo, Zmaj od Bosne bb, 71000 Sarajevo, Bosnia and Herzegovina
[b] Faculty of Electrical Engineering and Computing, University of Zagreb, Unska 3, 10000 Zagreb, Croatia

ARTICLE INFO

Article history:
Received 5 January 2017
Received in revised form 31 May 2017
Accepted 28 July 2017

Keywords:
Power systems
Power quality
Harmonic estimation
Kron reduction matrix
Optimization evaluation genetic algorithms
Sensitivity analysis

ABSTRACT

In this paper, a new algorithm for harmonic state estimation in power systems is represented. The algorithm is based on node voltage method, Kron reduction matrix, modeling of power system in frequency domain using phase values and optimization genetic algorithm. The algorithm uses measured voltage and current harmonics as an input data, with partially known data about transmission network. Algorithm estimates RMS and angle values of voltage harmonics in the unmonitored part of power system. Sensitivity analysis of proposed algorithm was conducted on a case study of 110 kV transmission network. Admittance matrix of power system is identified by using genetic algorithm with an accuracy of 0.5%, while an error of harmonic voltage estimation is lower than 1.129%.

1. Introduction

PSs represent the most complex techno-economical systems of today. For an efficient management of PS, basic requirement is efficient monitoring. High demanding life standards, application of optimization processes to improve efficiency, productivity and cost effectiveness of PSs are reasons why increasing number of PSs nowadays work near stability limit.

Current situation and future activities in the field of PQ are topics of concern of numerous working groups, research centers and science gatherings. In the papers [1–3] authors have presented a detailed overview of PQ monitoring. They concluded that harmonic monitoring represents a very important factor for cost effective techno-economical functioning of a PS. PQ monitoring at one point of PS gives information solely about PQ at the monitored point. On the other hand, estimation of PQ parameters in PS gives a global picture of PQ in observed PS. References [4,5] contain overview of methods, procedures and algorithms of PQ estimation in PS.

At the beginning of 70's a term "harmonic estimation" was introduced [6] and since then harmonic estimation remains topic of interest.

Causes of harmonic propagation in transmission networks, algorithm for HSE and mathematical formulation of higher harmonics in frequency domain are given in reference [7]. References [8,9] have similar approach to conducting HSE. In the reference [8] harmonics were analyzed, i.e. classic HSE, while in the reference [9] sub-harmonic state estimation was analyzed. In both references a node voltages method, Kron reduction matrix and problem solving in system of phase values were used. A proposed algorithm in references [8,9] was implemented on real PS configuration.

Most of the algorithms are based on node voltages method, however, algorithms implementing Kirchhoff's current law can be encountered as well. In the reference [10] Kirchhoff's current law was used, i.e. measurement of currents of buses. Certain simplifications were introduced and fitness function was formed. Maximum HSE error was 0.5% which is a good result.

Generally speaking, usage of LS, TLS, WLS, FDWLS and SVD in HSE represents basics of algorithms. Reference [11] used TLS and statistical approach to HSE results processing, and moreover, it discussed IEEE case study containing 14 buses. In the reference [11] for HSE were used WLS, SVD i FDWLS. Listed algorithms were implemented on two examples with real PS measurements. Furthermore, application of SVD in HSE was also explained in the reference [12,13]. By implementation of different approaches to HSE, so-called hybrid algorithms were developed, one of them being OA-HSE. OA-HSE was mathematically formulated and published in [14]. The algorithm is often cited in papers listing probability as one of the approaches to HSE. Furthermore, in reference [14], an example was given with real measurements made in PS. In the paper [15], authors used probability of certain harmonics occurrence at unmonitored PS buses in order to estimate harmonic state. Fur-

* Corresponding author.
E-mail addresses: vbecirovic@etf.unsa.ba (V. Bečirović), ivica.pavic@fer.hr (I. Pavić), bozidar.filipovic-grcic@fer.hr (B. Filipović-Grčić).

http://dx.doi.org/10.1016/j.epsr.2017.07.029
0378-7796/

Nomenclature

BGA	binary genetic algorithm
CT	current transformer
EMTP-RV	electromagnetic transient program – RV
FDWLS	fast decoupled weighted least square
GA	optimization evaluation genetic algorithms
GPS	global positioning system
HDA	harmonic domain algorithm
HS	harmonic sensitivity
HVN	height voltage networks or HV networks
LS	least square
LVN	low voltage networks or LV networks
MHS	mean harmonic sensitivity
MHVC	monitoring harmonic voltage and current – bus
MVN	medium voltage networks or MV networks
OA-HSE	observability analysis – HSE
PMU	phasor measurement unit
PQ	power quality
PS	power system
RMS	root mean square
SVD	singular value decomposition
TLS	total least squares
TVE	total vector error
VHE	voltage harmonic estimation – bus
VT	voltage transformer
WLS	weighted least square

thermore, IEEE case study containing 14 buses was discussed and criteria for HSE assessment, i.e. for HSE evaluation, were introduced in the same paper. Similarly, in 1998 paper [16] was published where concept of HSE application in PS was stated. It is interesting to compare ideas proposed in the past with their nowadays implementation. Certain proposals are today outdated in terms of new technologies.

HSE is often used as a tool to identify a harmonic source. In reference [17] an algorithm was presented for harmonic source identification in PS using LS for HSE. Moreover, in [18] HSE was also used for identification of harmonic sources and time synchronized measurement. GPS technology was implemented. The problem was analyzed in system of phase values.

All previously stated algorithms assume that input data are harmonics (voltage or current harmonics) of monitored PS buses. However, measurement instruments can give measurement data in form of power per each harmonic. In reference [19], a power flow calculation method HDA in frequency domain was given. The method is based on Newton-Raphson method, Norton's theorem and Kron reduction matrix.

In reference [20], GA was used for HSE, more accurately BGA was used for SVD. This paper discusses optimal positioning of PQ monitoring devices, and moreover it uses WLS for forming fitness function. A new approach to positioning of PQ devices was presented and the approach was implemented on IEEE case study containing 14 buses [20].

Majority of algorithms proposed or used nowadays for HSE are based on PMU technology. Furthermore, in the book [21] a mathematical formulation of PMU technology is given. In reference [22,23] PMU technology, along with ridge estimation, was used for HSE. Estimation error was determined by LS and satisfying results were obtained.

Through previous analysis of relevant literature and revision of papers from 2005 [24], 2011 [25] and 2013 [26], several important factors were established for analysis in process of HSE algorithms application: (1) based on what data and how fast HSE can be conducted, and moreover, what is expected accuracy of the algorithm; (2) Mathematical formulation of the problem, i.e. on what theoretical principles the algorithm is based; (3) models of certain PS elements (transmission line, power transformer, power electronics, power sources and loads); (4) applicability of certain optimization tools; (5) analysis in different domains (frequency and time domain). Through literature analysis Frances C. Arrillaga can be singled out as first person who introduced HSE algorithm, and as a result, a majority of papers rely on Arrillaga's researches.

Research presented in this paper is a continuation of the ones shown in the reference [27]. The goal of this paper is to show a detailed mathematical description of proposed HSE algorithm, to explain its characteristics and to conduct sensitivity analysis.

2. Problem statement

Efficient operation of PS is directly related to influences of harmonic propagation in PS. Harmonic propagation throughout power network and voltage distortion are directly transmitted from transmission power network to MVN and LVN. Philosophy of management and operation of HVN with goal of PQ improvement is the basis of reliable, stable and economically feasible transmission management. Higher harmonics cause the following effects in transmission networks: additional heating and losses of PS elements (transmission lines, transformers, compensation devices), unwanted voltage distortion, interference with railway systems, increased or decreased voltage levels, increased flow of circulating currents through grounding wire, decrease of transformer rated power, interference with conventional telecommunication lines, etc.

According to the procedure for harmonic measurement shown in IEC61000-4-7 [28], it is possible to analyze harmonic content using RMS and angle measurements (harmonic phasor). Other approaches to post-processing of waveforms for determining the harmonic content exist as well, such as application of wavelet-packet transform [29]. Majority of conventional PQ monitoring devices usually measure the average RMS values of recorded waveforms, while neglecting the angle. Stated neglection is a consequence of lack of angle analysis in standard EN50160 discussing PQ. If current and voltage harmonic phasors are treated using PMU technology [21], result are synchronized harmonic phasors. Application of algorithm for PMU ensures elimination of phase error from harmonic phasors. Post-processing of voltage and current waveforms on MHVC buses (Fig. 1) is based on IEC61000-4-7 [28] and then on algorithm for PMU technology [30,21].

Certain data about PS structure are usually unknown and therefore they represent a major problem for efficient HSE. Certain HSE algorithms having high accuracy assume that matrix [**Y**] is known.

In this paper, an algorithm is proposed which is applied to the transmission network of a single voltage level. This paper has two goals of research: (1) proposed HSE algorithm should enable faster and simpler modeling of PS based on a partially known data about PS; (2) algorithm should estimate harmonics on all buses with the same accuracy.

Sensitivity analysis is applied to determine how many results are within the range of acceptable (satisfying) values in terms of global matrix [$\mathbf{Y}(h)$] identification.

3. Harmonic state estimation

In the following chapters, an algorithm for HSE on PS buses without harmonic monitoring is mathematically and graphically described. An algorithm is based on: node voltages method, Kron reduction matrix, modeling of PS in the system of phase values,

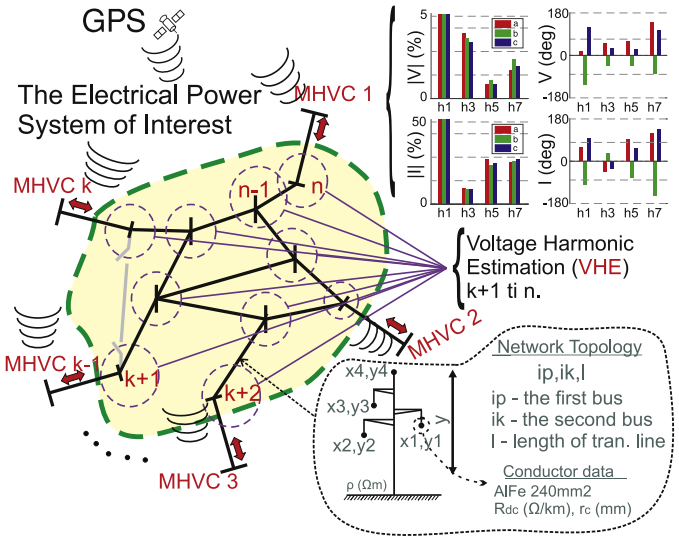

Fig. 1. Graphic interpretation of the problem.

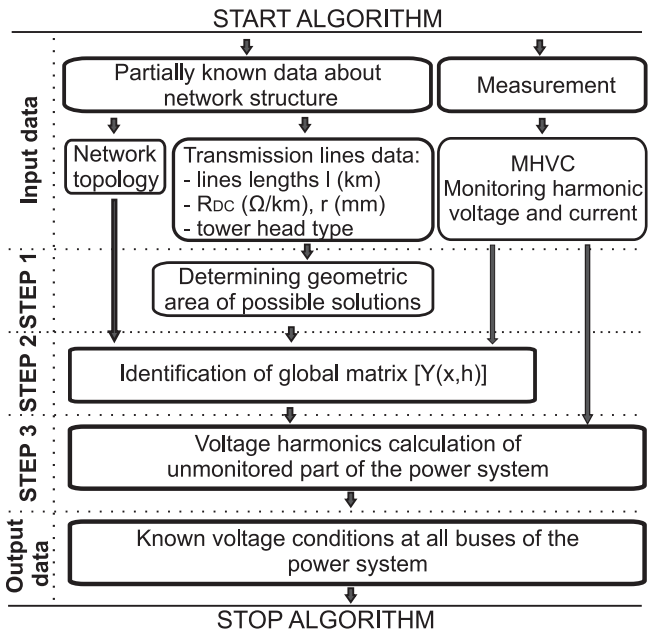

Fig. 2. Flowchart of proposed algorithm for estimation of voltage harmonics in unmonitored part of PS.

a matrix in the set of complex numbers, optimization GA and PS analysis in the frequency domain.

The problem of higher harmonics estimation in unmonitored part of PS can be defined in a following way:

Definition 1. For known network topology, know transmission line lengths, partially known structure of transmission line tower heads and known harmonic content in voltage and current waveforms at places of electrical energy exchange (MHVC buses), it is needed to estimate voltage harmonics at unmonitored points of power system (VHE buses).

Definition of a MHVC bus:

Definition 2. Buses having a monitoring of harmonic magnitude and angle are called harmonic monitoring buses (MHVC).

Definition of a VHE bus:

Definition 3. Buses without generation or consumption of electrical energy are buses of interest for voltage harmonic estimation (VHE).

3.1. Graphic interpretation of the problem

Graphic interpretation of the problem is shown in Fig. 1. In order to simplify problem interpretation, the problem is displayed using single-phase diagrams. The PS part surrounded (closed in terms of power) by harmonics monitoring devices, is shown in Fig. 1. Observed network has n buses in total, i.e. $3n$ nodes when it is observed in a system of phase values. Buses 1 to k have installed MHVC devices, while buses $k+1$ to n do not have consumers or generators of electrical energy. This is a general case with no limitations in terms of number of buses where voltage harmonic estimation should be conducted.

3.2. Input data

Necessary data for implementation of the proposed algorithm introduced in the following chapters of this paper, can be divided into two groups. (1) Buses MHVC are PS points (three phase buses) at which devices for harmonic monitoring are permanently installed. Mentioned devices measure RMS values and angles of harmonics, as shown in the upper right part of Fig. 1. It should be noted that devices positioned on MHVC buses must be time synchronized and this is usually done by using GPS system. (2) For the implementation of algorithm the following data must be known: network topology, transmission lines lengths, data about transmission line conductors (conductor type, R_{DC} (Ω/km), conductor radius r_c (mm)), type of transmission tower head (cat-head type, Y-tower, portal, triangular). It is not necessary to know the exact topology of transmission tower head.

Based on partially known data about part of the power network, it is not possible to form global matrix [**Y**], and therefore this matrix is unknown.

The mentioned matrix is formed for every harmonic of interest and is a function of transmission tower head geometry, transmission line length, switching status of the network and soil resistivity. Based on Fig. 1 and the definition of the problem, it can be concluded that global matrix [**Y**(x, h)] is function of vectors [x] and [h], where [x] is an independent variable (geometric parameters of transmission tower head and soil resistivity) and [h] is a vector of harmonics. Independent variable [x] by it's nature has limits that are function of transmission tower head and soil type along the transmission line route.

3.3. Proposed algorithm for HSE

Flowchart of the proposed algorithm shown in Fig. 2 describes the structure of input data, calculation process and structure of output data. This problem is mathematically formulated and solved in the following three steps: (1) Determining geometric area of possible results, i.e. determining limit values of independent variable [x]. This is an optimization problem and for its solving *Matlab Optimization Toolbox, Constrained Optimization and method fmincon* are used. The method *fmincon* searches independent variables in goal of minimizing the fitness function. (2) Identification of global matrix [**Y**(h)] of monitored and unmonitored parts of PS. The changes made are basically reduced to the calculation of independent variable [x], and then calculation of global matrix [**Y**(h)] for harmonics of interest. To determine an independent variable [x] GA optimization tool is used. (3) Based on the identified global matrix [**Y**(h)] and measurements from MHVC buses, harmonics of VHE buses (buses 1 to k in Fig. 1) are determined.

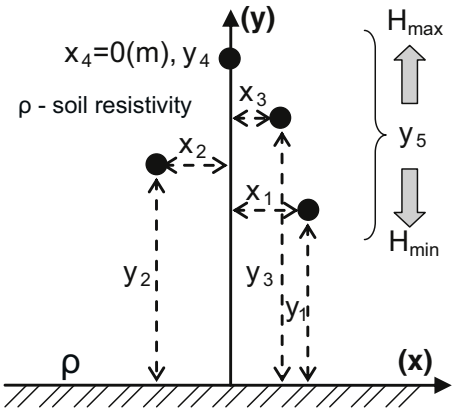

Fig. 3. Graphic interpretation of unknown variables.

3.4. Determining geometric area of possible solutions

Graphic interpretation of unknown variables is shown in Fig. 3. Initial estimated values are depicted in Fig. 3, and their values are either taken from project documentation or are standard values for the discussed voltage level and transmission tower head type. Geometric parameters and soil resistivity of transmission line can vary along its corridor. Therefore, geometric area of possible results needs to be calculated. This area corresponds to the area of possible physical results with all mechanical and electrical limits taken into account. If minimal distance $d_z(m)$ among all conductors is defined, radius around every conductor needs to be determined. Graphic interpretation of this problem is given in Fig. 4a). The problem of calculating $r_1 \ldots r_4$ becomes significantly more complicated by introducing parameter d_z. Moving all the parameters along the abscissa (x-axis) can lead to certain overlaps and multiple results with same values. As it is shown in Fig. 3, one parameter can be fixated and in this case a displacement of grounding conductor along the abscissa axis is selected, therefore $x_g = x_4 = 0\,(\mathrm{m})$.

Fitness function (1) is formed and mathematical limits (2) and (3) are introduced. The sum of circle surfaces with centers in initial points (x_i, y_j) $i = \overline{1,4}$, $j = \overline{1,4}$ must be maximum, and minimum distance between two conductors must be less or equal to set value $d_z(m)$. Furthermore, one more limitation is introduced, circle radius around grounding wire must be minimum $r_4 \leq min([r_1, r_2, r_3])$.

$$f(r) = (-1) \cdot \pi \cdot \sum_{i=1}^{4} r_i^2 \tag{1}$$

Starting from the expression (2) for calculation of distance between two points and by introducing already mentioned limitations (3) and (4) mathematical definition of the problem is created.

$$d_{ij} = \sqrt{(x_i - x_j)^2 + (y_i - y_j)^2};\ i \neq j,\ i,j = \overline{1,4}. \tag{2}$$

Based on Fig. 4 it is possible to define a system of inequalities that should be introduced as limitations in order to determine circle radius around every conductor.

$$r_i + r_j + d_z \leq d_{ij},\ i \neq j,\ i = \overline{1,4}.,\ j = \overline{1,4}. \tag{3}$$

Grounding wire, in formation process of substitute scheme in system of phase values, is eliminated from matrix of serial impedance and ground capacitance. By doing so, no omissions or simplifications are made [31–33].

$$r_4 - r_i \leq 0,\ i = \overline{1,3}. \tag{4}$$

It is necessary to determine minimum of function $f(r)$ (1) with limitations (2) and (3) wherein vectors of independent variable limit values $[r]$ are given by following expressions $r_{min} = [0]$, and $r_{\max} = [\max(d_{mn})]$, $m = \overline{1,4}.$, $n = \overline{1,4}$. Optimization results are radii of circles shown in Fig. 4a). By inscribing squares into circles, as shown in Fig. 4b), limits of possible solutions can be mathematically determined, as shown in expression (5).

$$\begin{aligned} x_{\min_i} &= x_i - \frac{r_i}{\sqrt{2}}; \quad y_{\min_i} = y_i - \frac{r_i}{\sqrt{2}}; \\ x_{\max_i} &= x_i + \frac{r_i}{\sqrt{2}}; \quad y_{\max_i} = y_i + \frac{r_i}{\sqrt{2}}. \end{aligned} \tag{5}$$

As it is possible to have a significant error on y-axis while choosing the initial points, one more variable is introduced Y_h, as demonstrated in Fig. 4c). This variable compensates geometric error of wrongly chosen initial points on y-axis. Based on soil configuration, sag, ambient temperature, points of hanging and weather conditions, it is not possible to accurately determine initial points on y-axis. Problem is solved by introducing parameters H_{min}, H_{max} representing geometric limitations of transmission tower head movement.

Soil resistivity $\rho\,(\Omega\mathrm{m})$ is one of the input data when having a goal of global matrix identification $[\mathbf{Y}(x, h)]$, and therefore it is necessary

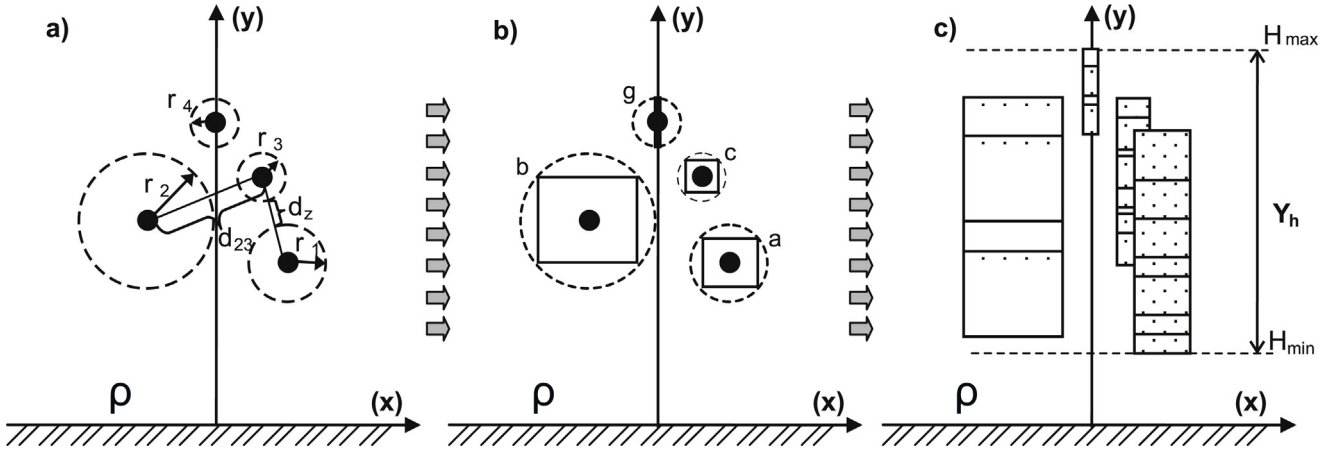

Fig. 4. Graphic interpretation of area of interest for calculation of possible results (a) determining area of possible results, (b) more rigorous criteria introduction and (c) area of possible results.

to define the borders of possible results. Soil resistivity can vary along the transmission line corridor and it depends on soil type. In this paper, one "equivalent" soil resistivity for every transmission line or more transmission lines is determined. Based on soil type, value of soil resistivity varies within the certain limitsthat can be found in the references [34–36].

The influence of soil resistivity is discussed in the reference [37]. High level of correlation between soil resistivity and electrical parameters of the transmission line is shown.

3.5. Identification of global matrix [**Y**(x, h)]

The problem is analyzed in the system of phase values, and furthermore, a global matrix [**Y**(*x*, *h*)] is unknown. Calculations of transmission line parameters are made based on references [32,33,38,39,37]. For substitute scheme of transmission line formation, three-phase π elements connected in series are used. Three-phase π elements are frequency dependent and a total number of elements is a function of frequency of interest and length of transmission line [40]. For analyses conducted in this paper, the highest frequency of interest is 10 kHz.

Three-phase Exact Pi-model of transmission line is realized based on references [41,42].

For identification of global matrix [**Y**(*x*, *h*)] one or more harmonics can be used. Harmonics currently present in the observed network must be chosen in order to avoid significant error in the identification. By applying the node voltage method, a following matrix can be written in the system of phase values for harmonics of interest [*h*] and vector of unknown values [*x*] (vector of geometric parameters and soil resistivity):

$$[\mathbf{Y}(x,h)]\cdot[\mathbf{V}(h)]=[\mathbf{I}(h)]. \tag{6}$$

Vectors [**V**(*h*)] and [**I**(*h*)] are partially known and *k* is a number of known elements. Previously defined system of matrix equations (6) can be written in the following form:

$$\begin{bmatrix}[\mathbf{Ys}_{1,1}] & [\mathbf{Ys}_{1,2}]\\ [\mathbf{Ys}_{2,1}] & [\mathbf{Ys}_{2,2}]\end{bmatrix}\cdot\begin{bmatrix}[\mathbf{Vs}_1(h)]\\ [\mathbf{Vs}_2(h)]\end{bmatrix}=\begin{bmatrix}[\mathbf{Is}_1(h)]\\ [\mathbf{Is}_2(h)]\end{bmatrix}. \tag{7}$$

Vectors [$\mathbf{Vs}_1(h)$] and [$\mathbf{Is}_1(h)$] represent measured values of voltage and current harmonics in the monitored part of the PS. Vector [$\mathbf{Vs}_2(h)$] represents unknown vector of voltages, i.e. vector of estimated harmonic values in the unmonitored part of PS. Vector [$\mathbf{Is}_2(h)$] = [0], because in the unmonitored part of PS there is no production or consumption in process of global matrix [**Y**(*h*)] identification. Based on a condition [$\mathbf{Is}_2(h)$] = [0], and furthermore, based on Kron reduction matrix [43–47], a reduction of global matrix [**Y**(*x*, *h*)] is performed by using an expression (7):

$$[\mathbf{Yr}(x,h)]=[\mathbf{Ys}_{1,1}]-[\triangle\mathbf{Ys}_{1,1}], \tag{8}$$

where:

$$[\triangle\mathbf{Ys}_{1,1}]=[\mathbf{Ys}_{1,2}]\cdot[\mathbf{Ys}_{2,2}]^{-1}\cdot[\mathbf{Ys}_{2,1}]. \tag{9}$$

Reduced matrix [**Yr**(*x*, *h*)] is of $k\times k$ size, it is a function of vector [*x*] and moreover it inherits all its characteristics from global matrix [**Y**(*x*, *h*)] [43,45,48], thus no simplifications are made. Reduced matrix (8) and vectors [$\mathbf{Vs}_1(h)$], [$\mathbf{Is}_1(h)$] form a following equation:

$$[\mathbf{Yr}(x,h])\cdot[\mathbf{Vs}_1(h)]=[\mathbf{Is}_1(h)]. \tag{10}$$

Elements of reduced matrix are functions of independent variable [*x*] and [*h*].

$$[\Lambda(x,h)]=[\mathbf{Yr}(x,h)]\cdot[\mathbf{Vs}_1(h)]-[\mathbf{Is}_1(h)] \tag{11}$$

Elements of vector [$\Lambda(x,h)$] are complex numbers $\gamma_i(x,h)\ i=\overline{1,k}$. and they represent an identification error. According to the rules of metric for complex numbers [49], a following equation can be written:

$$f(x,h)=\sum_{i=1}^{k}|\gamma_i(x,h)|. \tag{12}$$

In a case when global matrix identification [**Y**(*h*)] is determined for multiple harmonics, a following fitness function is formed:

$$F(x)=\min_x\Big(\sum_{i=1}^{H}Kp_i\cdot f(x,h_i)\Big), \tag{13}$$

where *Kp* is a weighting factor for harmonics and is part of R_0^+ set of numbers and *H* is length of vector [*h*]. Minimum of function *F*(*x*) determines independent variables [*x*]. Expression (13) represents the fitness function and optimization algorithm should be applied to it. When vector [*x*] is calculated with satisfying accuracy and limitations, then model of the network is known.

3.6. Identification error analysis

Global matrix [**Y**(*x*, *h*)] is calculated with satisfying accuracy [$\varepsilon_I(h)$] = [$\Lambda(x,h)$]. Result of global matrix [**Y**(*x*, *h*)] identification is vector [*x*]. If vector [*x*] is eliminated from the expression (10) (because it was already calculated) and elimination error is taken into account, then a matrix equation, per each harmonic for which identification was carried out, is obtained.

$$[\mathbf{Yr}(h)]\cdot[\mathbf{Vs}_1(h)]=[\mathbf{Is}_1(h)]+[\varepsilon_{I_1}(h)] \tag{14}$$

Vector [$\varepsilon_{I_1}(h)$] is a complex vector of node current correction and is equal to identification error. As a consequence of identification, complex vector of node current correction [$\varepsilon_{I_2}(h)$] of unmonitored buses in observed PS exists.

$$[\varepsilon_I([h])]=\begin{bmatrix}[\varepsilon_{I_1}(h)]\\ [\varepsilon_{I_2}(h)]\end{bmatrix} \tag{15}$$

Vector [$\varepsilon_{I_2}(h)$], besides being unknown, represents a problem since there is no existing load on unmonitored buses. With intent to eliminate vector [$\varepsilon_{I_2}(h)$], and consequently by eliminating vector [$\varepsilon_{I_1}(h)$], complex vector of node voltages correction [$\varepsilon_{V_1}(h)$] is introduced, resulting in the new form of expression (14).

$$[\mathbf{Yr}(h)]\cdot([\mathbf{Vs}_1(h)]+[\varepsilon_{V_1}(h)])=[\mathbf{Is}_1(h)] \tag{16}$$

Expressions (14) and (16) are derived from expression (10) and identification error. Consequence of introducing a node voltage correction complex vector [$\varepsilon_{V_1}(h)$] is an error introduction into voltage calculation of unmonitored buses, i.e. node voltage correction complex vector [$\varepsilon_{V_2}(h)$] of unmonitored PS buses must be introduced. Link between vectors [$\varepsilon_{V_1}(h)$] and [$\varepsilon_{V_2}(h)$] is defined by the following expression:

$$[\varepsilon_{V_2}(h)]=-[\mathbf{Zs}_{2,2}(h)]\cdot[\mathbf{Ys}_{2,1}(h)]\cdot[\varepsilon_{V_1}(h)] \tag{17}$$

It should be noted that in the above expression [$\mathbf{Zs}_{2,2}(h)$] = [$\mathbf{Ys}_{2,2}(h)$]$^{-1}$. Moreover, according to expression (16), [$\varepsilon_{V_1}(h)$] can be written in a following way [$\varepsilon_{V_1}(h)$] = [$\mathbf{Yr}(h)$]$^{-1}\cdot$[$\mathbf{Is}_1(h)$] − [$\mathbf{Vs}_1(h)$]. Node voltages correction vector [$\varepsilon_{V_2}(h)$] of unmonitored PS buses obtains a new form:

$$[\varepsilon_{V_2}]=-[\mathbf{Zs}_{2,2}]\cdot[\mathbf{Ys}_{2,1}]\cdot([\mathbf{Zr}]\cdot[\mathbf{Is}_1]-[\mathbf{Vs}_1]) \tag{18}$$

In the above formula, [$\mathbf{Zr}(h)$] = [$\mathbf{Yr}(h)$]$^{-1}$. In order to maintain discussed problem in form of node voltage method [**Y**]·[**V**] = [**I**], correction of node voltages vector must be made. Thus, term of voltage conditions of unmonitored PS buses correction vector is introduced.

$$[\mathrm{Vs}_1^{(k)}(h)]=[\mathbf{Vs}_1(h)]+[\varepsilon_{V_1}(h)] \tag{19}$$

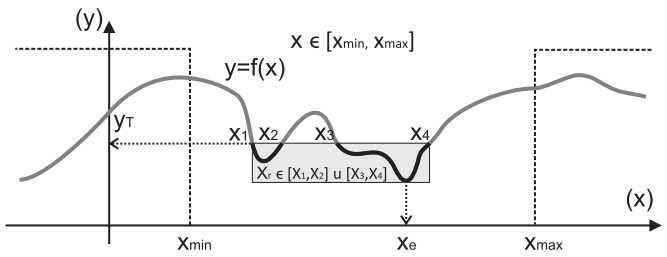

Fig. 5. Graphic illustration of the problem along with the set of satisfying results.

New matrix equation (20) is formed based on expression (7). The equation is suitable for further implementation when calculating voltage conditions at unmonitored PS buses in case without generating or consuming units attached to it.

$$\begin{bmatrix} [\mathbf{Ys}_{1,1}] & [\mathbf{Ys}_{1,2}] \\ [\mathbf{Ys}_{2,1}] & [\mathbf{Ys}_{2,2}] \end{bmatrix} \cdot \begin{bmatrix} \left[\mathbf{Vs}_{\mathbf{1}}^{(\mathbf{k})}\right] \\ [\mathbf{Vs}_2] + [\varepsilon_{V_2}] \end{bmatrix} = \begin{bmatrix} [\mathbf{Is}_1] \\ [\mathbf{Is}_2] \end{bmatrix} \tag{20}$$

3.7. Calculation of voltage harmonics in the unmonitored part of power system

By applying the Kron reduction matrix on the expression (20) voltage conditions of unmonitored buses get a form of:

$$[\mathbf{Vs}_2] + [\varepsilon_{V_2}] = [\mathbf{Ys}_{22}]^{-1} \cdot \left([\mathbf{Is}_2] - [\mathbf{Ys21}] \cdot \left[\mathrm{Vs}_{\mathbf{1}}^{(\mathrm{k})}\right] \right) \tag{21}$$

Buses number $k+1$ to n do not have generating nor consumption units connected to it, therefore node currents vector for these buses is a zero vector $[\mathbf{Is}_2([h])] = [0]$. Matrix equation (21) can be expressed as:

$$[\mathbf{Vs}_2] + [\varepsilon_{V_2}] = -[\mathbf{Ys}_{22}]^{-1} \cdot [\mathbf{Ys}_{21}] \cdot \left[\mathrm{Vs}_{\mathbf{1}}^{(\mathrm{k})}\right]. \tag{22}$$

Vector $[\varepsilon_{V_2}(h)]$ is obtained by using expression (18) and when it is included into expression (22), voltage vector of unmonitored buses is determined by using the following expression (23).

$$[\mathbf{Vs}_2(h)] = -[\mathbf{Ys}_{22}(h)]^{-1} \cdot [\mathbf{Ys}_{21}(h)] \cdot [\mathbf{Vs}_1(h)] \tag{23}$$

4. Sensitivity analysis

Sensitivity analysis is carried out to determine how many results are within the limits of acceptable values in terms of global matrix $[\mathbf{Y}(h)]$ identification. In order to simplify an explanation of the problem, it is assumed that the problem is solved in 2D space. The segment $[x_{min}, x_{max}]$ is established by geometric area of possible results Section 3.4. Set of acceptable results is defined by satisfying accuracy ε, and ε is obtained using [28,50]. For a given function $f(x)$, as one in Fig. 5, satisfying set of results is:

$$f(x_e) \leq f(x_r) \leq y_T \tag{24}$$

where $y_T = f(x_e) + \varepsilon$, a $x_r \in [x_1, x_2] \cup [x_3, x_4]$.

4.1. Mathematical formulation of sensitivity analysis

Set of input data is uniformly generated within the area shown in Fig. 4c) according to [51] (linear generator), matrix $[X] = ||x_{t,q}||$, $[X] \in \mathbb{R}$. Counter t represents set of data in process of sensitivity analysis, $t = \overline{1, ne}$ where ne is total number of experiments. Counter q represents total number of variables $q = \overline{1, nv}$ where $nv = 9$ (example in Section 5). Initial vector $[x_{0,q}]$ (initial geometry of transmission tower head) is specified and then the diagonal matrix $[A]$ containing elements $\{0, 1\}$ and having dimensions of $nv \times nv$ is formed. Furthermore, an appropriate metric vector $[dX_t]$ with dimensions of $1 \times nv$ is also specified for every step t.

$$[x_{t,q}] = [x_{t-1,q}] + [A] \cdot [dX_t] \tag{25}$$

For uniformly predefined set of data, set of output data is obtained, 3D matrix $[\mathbf{W}] = ||\mathbf{w}_{t,b,h}||$, $[\mathbf{W}] \in \mathbb{C}$. Counter b represents total number of buses $b = \overline{1, nb}$, where for example in Section 5, $nb = 12$ (bus 4×3). Counter h represents total number of harmonics of interest $h = \overline{1, nh}$, where $nh = 4$ (example in Section 5). Measurements of voltage $[\mathbf{Vs}_1(h)]$ and current $[\mathbf{Is}_1(h)]$ harmonics are conducted on MHVC buses. Vector $[\mathbf{Vs}_1(h)]$ is used for determining set of output data, Algorithm 1. Based on vector $[\mathbf{Is}_1(h)]$, matrix $[\mathbf{Im}] = ||\mathbf{im}_{b,h}||$ $[\mathbf{Im}] \in \mathbb{C}$ is formed.

Algorithm 1. Algorithm for calculation of output data

```
t = 1, ne
  [x_{t,1:nv}] = [x_{t-1,1:nv}] + [A] · [dX_t]
h = 1, nh
[w_{t,1:nb,h}] = [Yr([x_{t,1:nv}], h)] · [V_{S_1}(h)]
  end
end
```

The set of output data is analyzed to evaluate sensitivity of the algorithm. Sensitivity analysis evaluation is performed in two steps. (1) Standard deviation of output data is calculated to determine sensitivity of tower head geometry change to harmonics and buses in PS [52]. (2) Identification accuracy is represented by average identification error per MHVC bus and per every harmonic.

4.2. Standard deviation

According to rules of metrics for set of complex numbers [49], standard deviation is given by expression (26).

$$\sigma_{b,h} = \sqrt{\frac{\sum_{t=1}^{ne} (|w_{t,b,h} - im_{b,h}|)^2}{ne}} \quad \begin{matrix} b = \overline{1, nb} \\ h = \overline{1, nh} \end{matrix} \tag{26}$$

Expression (26) is applied to all harmonics at all buses. A goal is to determine sensitivity of tower head geometry change to harmonics and buses in PS. Results obtained by applying the expression (26) to 110 kV power network are shown in Fig. 9.

4.3. Algorithm sensitivity

Sensitivity analysis is conducted on the set of output data (matrix $[\mathbf{W}]$) and it is compared with current amplitude measurements at MHVC buses. By forming histogram shown in Fig. 10 with default accuracy, percentage share of experiments in the nearby area of accurate value is determined. Default accuracy is arbitrary value and represents allowed error of global admittance matrix $[\mathbf{Y}(x, h)]$ identification. Percentage share of experiments satisfying default accuracy is calculated using a program code Listing 1. Graph in Fig. 11 shows result of the program code Listing 1 application to buses and current harmonics.

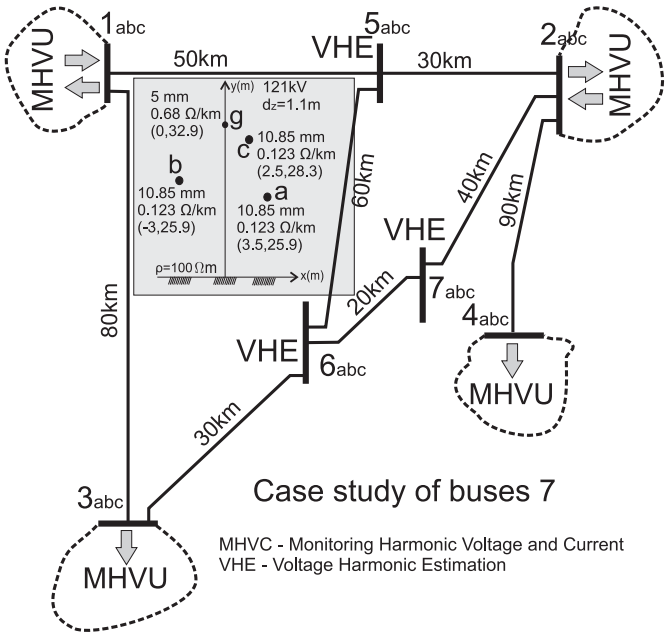

Fig. 6. Scheme of analyzed example (case study).

Listing 1. Evaluation function

```
function [result]=fcnEvaluation...
  (default_accuracy, samples,exact_value)
n=length(samples);
samples(n+1)=exact_value;
max_N=max(samples);
min_N=min(samples);
eps=default_accuracy*exact_value/100;
step=floor((max_N-min_N)/eps);
  if step==0
    result=100;
  else
    [sampl, value]=hist(samples,step);
    [mins s]=min(abs(value-exact_value));
    result=sampl(s)/sum(sampl)*100;
  end
end
```

By variation of default accuracy in range from 0.1% to 20% a set of data per buses and harmonics is obtained. For each value of variable default accuracy it is possible to determine sensitivity of certain harmonic at MHVC bus. HS is a parameter expressed in percentage and it shows how many experiments satisfy certain accuracy. HS considers only a single harmonic at a single bus. MHS is the average HS value. Graph in Fig. 12 is example of MHS.

5. Computational verification of proposed HSE

Current version of standard EN50160 [53] is applicable to voltage levels up to 150 kV. For a case study, a part of 110 kV transmission network was considered containing seven three-phase buses. Harmonic monitoring is present at four buses, while on the remaining three buses it is necessary to estimate voltage conditions, Fig. 6. Problem is modeled in a three-phase manner in EMTP-RV which contains frequency dependent transmission line model, whereas simulation is conducted in time-domain. During the simulation, frequency of fundamental harmonic remains the same and is equal to 50 Hz. Consumers connected to the buses 3 and 4 are generating higher harmonics, asymmetry and flickers into the network. Electrical energy is produced at buses 1 and 2.

Computational verification of the proposed HSE method was carried out in order to eliminate the effect of measurement errors caused by CT and VT on harmonic estimation results.

Fig. 6 shows configuration of the 110 kV power network with transmission lines lengths and transmission tower head type. Data about transmission tower head type are accurate values, however, the algorithm does not have those values on its disposal while identifying global matrix [**Y**]. It is assumed that all 110 kV transmission lines have the same tower head type and that for all conductors soil resistivity is 100 Ωm.

The problem is solved using algorithm from Fig. 2. In step 1, based on data from Fig. 6 and mathematical model from Section 3.4, Table 1 is formed. Table 1 represents one set of input data for identification of global matrix [**Y**(x, h)]. Parameter Y_h (Fig. 4c)) represents min/max displacement of transmission line head on y-axis.

Second set of input data are lengths of transmission lines that are given in Fig. 6. Third set of input data for identification of global matrix [**Y**(x, h)] are measurements made on MHVC buses. Post-processing of MHVC buses is conducted according to IEC61000-4-7 [28]. Calculated phasors per buses and per harmonics represent input data for the identification of global matrix [**Y**(x, h)]. Only odd harmonics are considered since analyses are conducted in steady state. In Fig. 7 input data are given for the identification of global matrix [**Y**(x, h)].

5.1. Sensitivity analysis of global matrix identification

Based on expression (25), a uniformly predefined set of geometric data is formed, Fig. 8. For every set of data, identification of global matrix [**Y**(x, h)] is conducted based on Table 2 shown in Appendix A. Obtained results are processed using the expression (26) and shown in Fig. 9. By comparison analysis of standard deviations, existence of high correlation level between all buses and corresponding harmonics can be noted. In other words, geometry variation equally affects all buses and corresponding harmonics. The stated leads to the conclusion that geometric area of possible solutions contains multiple acceptable (satisfying) results.

In total 21870 experiments (sets of input data) were made. Fig. 10 shows histogram for bus 1 (phase a) and fundamental current harmonic. Histogram is formed in case when accuracy of 1% is considered. This means that total number of experiments in the area of 1% of accurate value (default_accuracy = 1%, listing 1) is determined. 1972 experiments meet this accuracy, i.e. there is 9% chance that the result is the range of 1%.

Previously stated is conducted for all buses and harmonics. It can be concluded that current harmonics present on monitored PS buses have high correlation level between required accuracy and percentage share of satisfying experiment set. This shows that for efficient identification it is necessary to choose harmonics present in PS.

Efficient identification means furthermore efficient harmonic estimation. Identification error is determined by set of experiments

Table 1
Calculated geometric area.

Con.	r_c (mm)	R_{dc} (Ω/km)	$H_{min/max}$ (m)	x_{min} (m)	y_{min} (m)	x_{max} (m)	y_{max} (m)
1	10.85	0.123	±15	1.83	21.83	5.17	25.17
2	10.85	0.123		−5.45	23.45	−0.55	28.34
3	10.85	0.123		1.48	27.29	3.51	29.32
4	5	0.68		0.00	31.46	0.00	34.34

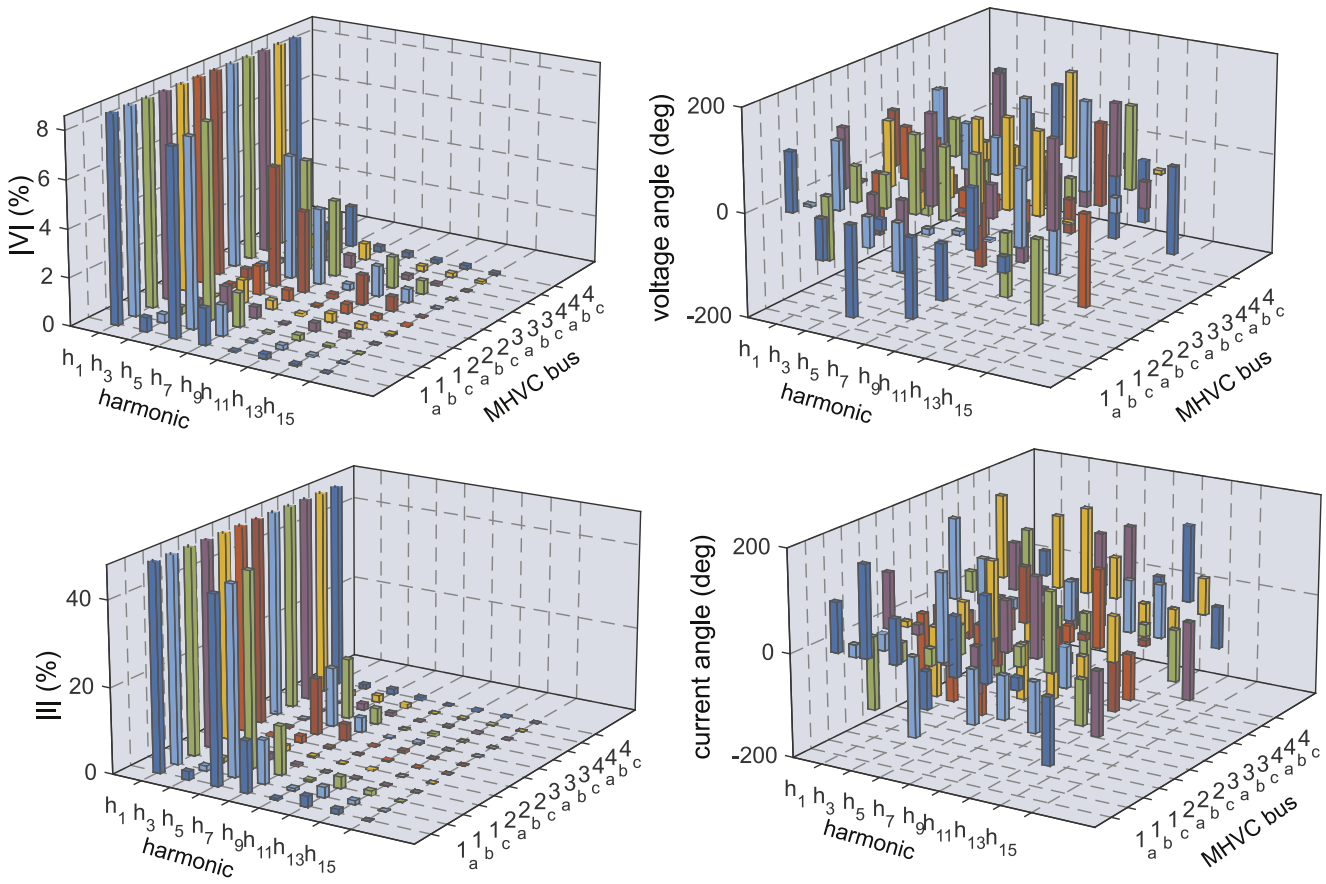

Fig. 7. Odd harmonics content (its percentage share compared to fundamental harmonic content) in voltage and current waveform on monitored busses of the PS.

having required accuracy. For each harmonic and bus a histogram is formed as shown in Fig. 10 for required accuracy of 0.1%. Percentage share of experiments set with satisfactory accuracy of 0.1% for all harmonics and buses is calculated.

Fig. 11 shows percentage of how many results is contained in total number of conducted experiments. From a graph shown in Fig. 11 it can be seen that harmonics present in the PS have 0.5% experiments satisfying accuracy of 0.1%. In this particular case those are harmonics $h = [\,1 \quad 5 \quad 7 \quad 11\,]$.

In Section 4.3 a procedure for obtaining the graph shown in Fig. 12 is described. In Fig. 12 two graphs are shown and based on these graphs an efficiency assessment of the optimization tool application is made. In the area of required accuracy from 0.1% to 1% MHS is of same trend for all buses. This area is also the goal area for the global matrix [**Y**] identification. The range from 1% to 20% has two goals: (1) to show that all global matrix [**Y**] identification results are in range of ca. 20% error, (2) to show that MHS is of the same trend for all buses.

5.2. Harmonic estimation at unmonitored part of power system

Identification was conducted for harmonics $h = \begin{bmatrix} 1 & 5 & 7 \end{bmatrix}$ using GA. From Fig. 13, significant errors in tower head geometry and soil resistivity evaluation can be noticed. It is not possible to use this algorithm for estimation of transmission line tower head geometry. An error in soil resistivity is 43.9%. Through repetition of calculations, multiple times mentioned error was in range of ca. 3.5% to 60%. In reference [54], graphs indicating possible influence of soil resistivity on parameters of substitute scheme in system of phase components are given. Positive and zero sequence substitute scheme of series impedance is analyzed. Frequency dependence of ground capacitance can be disregarded up to 1 MHz [32]. For positive sequence, parameters R_d and L_d are frequency independent till ca. 1 kHz. In zero sequence, parameter R_0 is independent till ca. 10 Hz, while parameter L_0 is frequency dependent in range DC to 10 MHz. Transmission lines discussed in this example are symmetrically loaded, or to be exact, there is asymmetry presence of ca. 1% to 2% depending on transmission line. Consequently, the presence of zero sequence is negligible, and thus the whole model is nonsensitive to major changes of soil resistivity.

For harmonic estimation GA was used. GA was chosen based on convergence speed criteria and finding of at least one local minimum satisfying certain accuracy. It cannot be ascertained that this is the most suitable optimization tool for this mathematical algorithm. However, it is shown that this algorithm obtains satisfying results. Maximum error in process of identification is ca. 3%, Fig. 14. In Fig. 12, an accuracy of ca. 0.5% can be read off for 3% error. From previous considered, it can be concluded that GA has forced accuracy of 0.5% in process of identification. This is not a bad result, however, much more accurate results do exist.

Results of voltage estimation for VHE buses is graphically depicted in Fig. 15 and in Table 3. Voltage estimation of VHE buses is conducted based on voltage conditions of MHVC buses. From expression (23) identification error is eliminated, thus making a HSE algorithm more efficient.

In the considered case study, system frequency during the simulation period was 50 Hz. If a system frequency was changed, it would have been necessary to post-process voltage and current waveforms of monitored buses according to algorithm for PMU

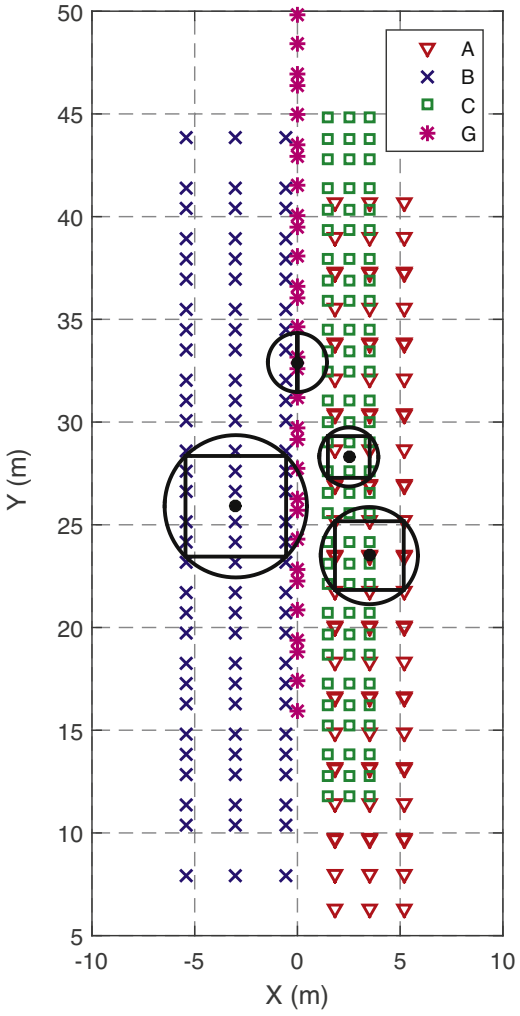

Fig. 8. Uniformly predefined set of geometric input data.

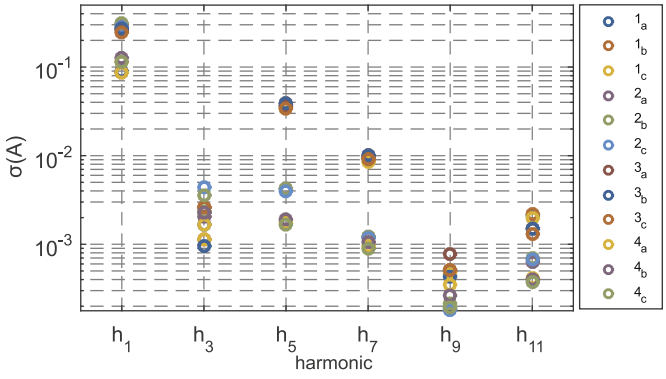

Fig. 9. Standard deviation of current harmonics at MHVC buses.

technology. One of the possible future researches is application of this algorithm to PSs dynamic system frequency.

5.3. Analysis of harmonic estimation error

As this paper discusses simulation model of the network, it is possible to compare accurate and estimated values of voltages on VHE buses. The comparison is made according to PMU algorithm for estimation of phasor TVE measurement error. TVE represents

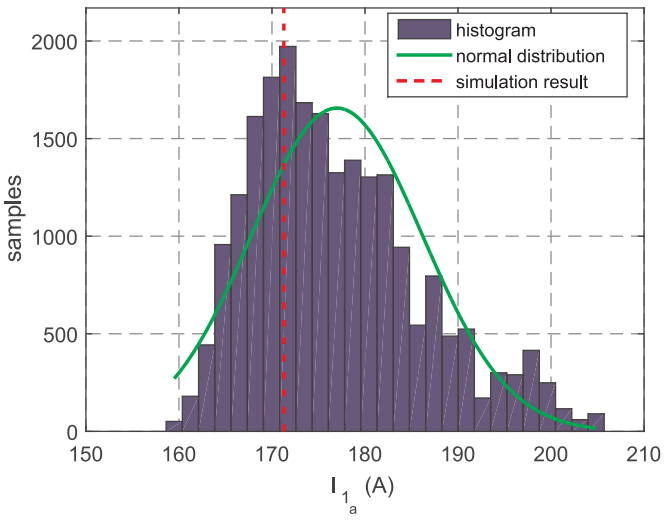

Fig. 10. Sample distribution of fundamental current harmonic on bus 1 (phase a) for accuracy of 1%.

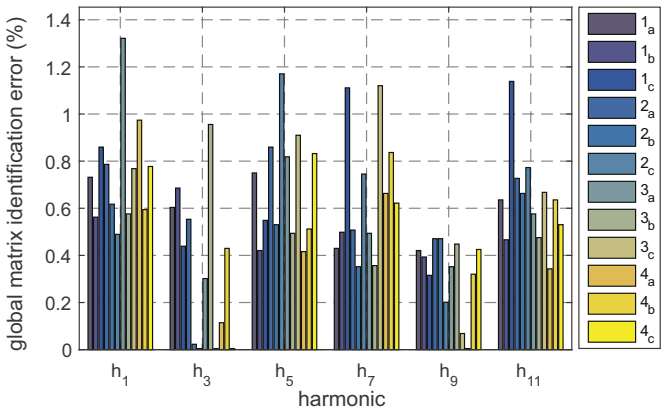

Fig. 11. Global matrix [**Y**(*x*, *h*)] identification error per current harmonics and buses for default accuracy of 0.1%.

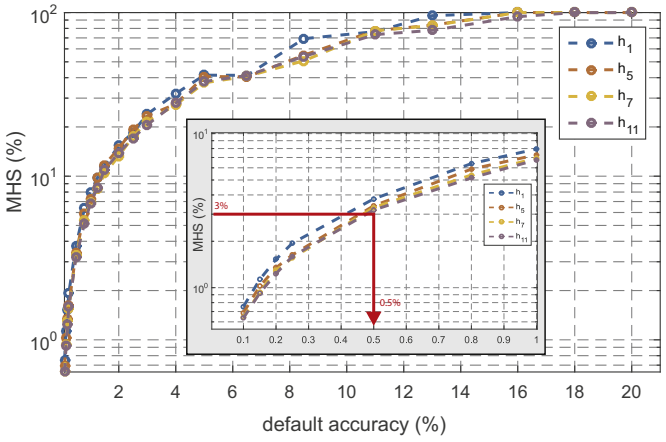

Fig. 12. MHS as a function of default error in the step of global matrix identification procedure [**Y**(*x*, *h*)].

stricter criteria compared to calculation of relative error of RMS harmonics.

Result of HSE algorithm application is given in Fig. 15 and Table 3. If simulation results and estimation results are compared, following errors can be seen: maximum error of 1.129% is noted on bus 7 of phase c for third harmonic; minimum error is noted on bus

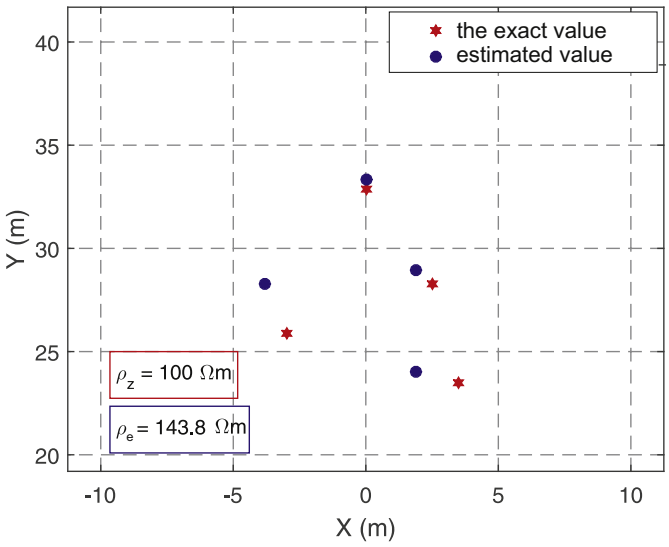

Fig. 13. Graphic interpretation of power line head for identified matrix [**Y**(*x*, [**h**$_1$**h**$_5$**h**$_7$])].

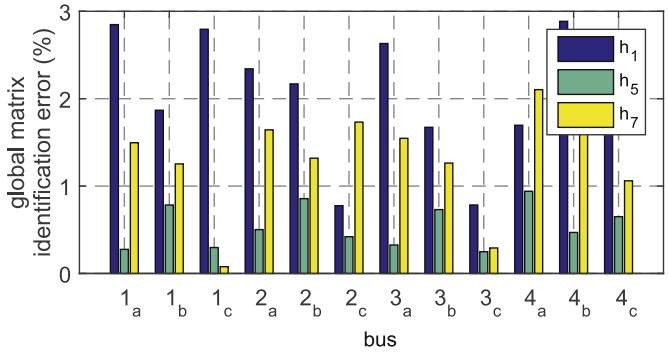

Fig. 14. Error of global matrix identification [**Y**(*x*, **[h**$_1$**h**$_5$**h**$_7$**]**)] using GA.

5 of phase b for first harmonic, and average error per harmonics and phases is 0.3%. By comparing identification and estimation error, it can be concluded that estimation error is lower.

From Fig. 16 it can be concluded that more than 98% of results has TVE lower than 1%. Majority of published papers considers relative error of harmonic estimation. By analysis of reference [55] it can be concluded that 63.3% results on all buses and harmonics have relative errors lower or equal to ±5%. According to reference [8], which is a basis for HSE, maximum relative harmonic estimation error is ±5%.

Reference [15] discusses IEEE system of 14 buses, and an average error of voltage estimation is ±6.25%. Researches demonstrated in reference [56] represent continuation of the research shown in [8], and average relative error per harmonics and buses is ca. ±6%. In reference [57], two methods are analyzed on two different examples: SVD and FDWLS in HSE. Analysis of harmonic estimation relative error as a function of number of unmonitored buses is conducted [57]. By analysis of results obtained from reference [57] it can be concluded that average error in case when over 40% buses are monitored in PS is smaller than ca. 4%. Reference [58] considers PS with 14 buses and analyzes three-phase harmonic distortion state estimation. Majority of errors are smaller than 4% and a maximum harmonic estimation error is 9%. Reference [59] considers HSE problem for distribution networks using PMUs. In reference [59] maximum harmonic estimation error is lower than 0.1%.

Based on analyzed literature it can be concluded that relative error of ±5% represents a challenge for nowadays HSE algorithms. In

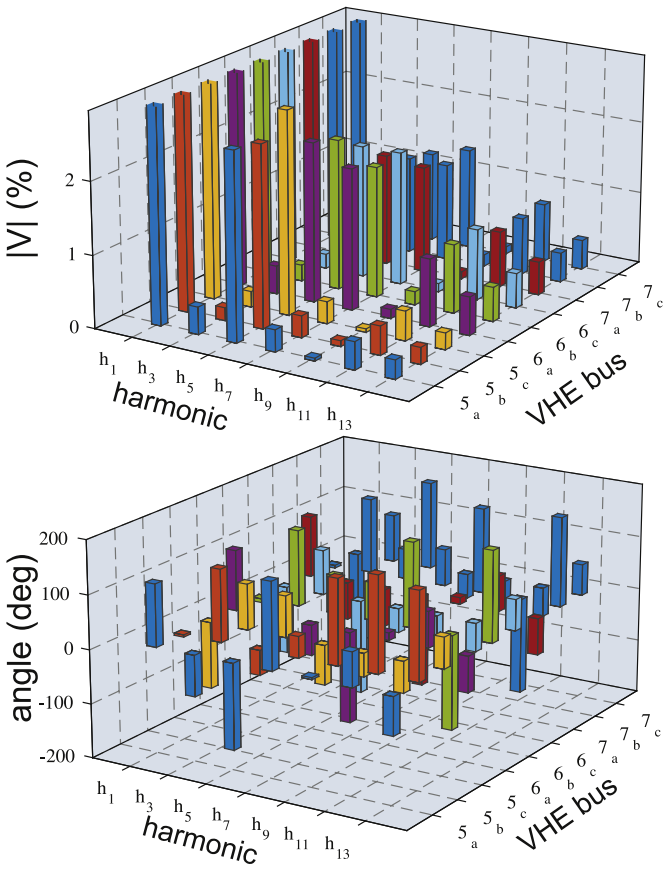

Fig. 15. Estimated voltage conditions at unmonitored PS buses.

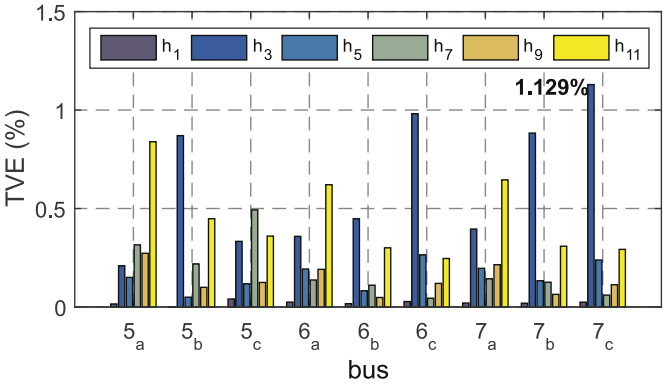

Fig. 16. Harmonic estimation error of unmonitored buses.

comparison to analyzed literature, errorsshown in this paper represent major improvement. It should be mentioned that scope of the problem, in comparison to literature, would be somewhat smaller. Criteria of HSE error could be obtained from PMU requirements. Parameter TVE on all buses and harmonics *TVE* ≤ 1% represents a challenge for certain HSE algorithms.

6. Future work

Overview of future researches and improvements of the presented algorithm: (1) In order to enhance the performances of a proposed algorithm, future research will have direction of algorithm implementation for selected harmonics based on which global matrix identification will be performed with goal of achieving high degree of accuracy. (2) Input data of algorithm can be a

Table 2
Tabular presentation of odd voltage and current harmonic content of monitored PS buses.

Bus	Label	Unit	h_1	h_3	h_5	h_7	h_9	h_{11}	h_{13}	h_{15}
1	$\|U_a\|$	kV	63.558	0.377	4.952	0.969	0.029	0.130	0.053	0.001
	$\angle\Theta_a$	deg	115.191	−79.582	−176.327	22.026	−153.156	−106.113	114.414	−29.541
	$\|I_a\|$	A	171.276	3.372	74.985	20.688	0.778	4.319	1.975	0.074
	$\angle\phi_a$	deg	96.577	178.552	87.426	−72.195	114.226	163.080	23.903	−127.773
	$\|U_b\|$	kV	63.280	0.228	4.983	0.816	0.043	0.120	0.043	0.002
	$\angle\Theta_b$	deg	−4.867	131.962	−59.543	−93.649	−10.980	7.637	3.105	145.293
	$\|I_b\|$	A	175.402	2.135	77.776	17.876	1.156	4.299	1.713	0.171
	$\angle\phi_b$	deg	−24.314	31.576	−155.272	169.500	−105.573	−84.078	−96.794	75.977
	$\|U_c\|$	kV	63.309	0.189	5.172	0.902	0.030	0.141	0.043	0.001
	$\angle\Theta_c$	deg	−124.691	69.336	64.474	150.630	137.883	134.879	−121.266	−161.059
	$\|I_c\|$	A	176.156	1.823	80.395	20.165	0.776	4.791	1.862	0.104
	$\angle\phi_c$	deg	−142.611	−36.147	−33.161	56.369	36.398	38.417	152.000	−87.036
2	$\|U_a\|$	kV	64.404	0.152	0.687	0.306	0.026	0.224	0.148	0.006
	$\angle\Theta_a$	deg	117.799	−77.195	−142.154	175.427	3.004	63.295	−72.109	170.900
	$\|I_a\|$	A	610.628	3.135	8.741	2.802	0.186	1.297	0.726	0.027
	$\angle\phi_a$	deg	109.946	19.215	−48.547	−92.141	98.935	154.667	19.772	−124.951
	$\|U_b\|$	kV	64.002	0.031	0.625	0.243	0.064	0.234	0.124	0.039
	$\angle\Theta_b$	deg	−2.359	127.296	−33.866	56.487	161.639	174.628	160.134	−4.215
	$\|I_b\|$	A	624.084	0.633	7.938	2.201	0.452	1.343	0.600	0.166
	$\angle\phi_b$	deg	−11.048	−136.706	59.615	149.399	−106.342	−93.512	−108.218	87.458
	$\|U_c\|$	kV	64.237	0.121	0.780	0.290	0.043	0.249	0.124	0.035
	$\angle\Theta_c$	deg	−122.423	101.170	87.860	−51.169	−30.382	−60.089	58.997	−179.770
	$\|I_c\|$	A	619.504	2.534	9.882	2.628	0.311	1.451	0.602	0.144
	$\angle\phi_c$	deg	−130.541	−162.922	−178.424	41.104	61.181	31.705	149.458	−88.007
3	$\|U_a\|$	kV	60.061	0.286	3.045	2.054	0.117	0.758	0.367	0.011
	$\angle\Theta_a$	deg	109.273	−62.693	−34.172	−165.839	16.953	69.346	−64.438	156.534
	$\|I_a\|$	A	554.459	1.827	74.079	21.677	0.764	2.925	0.698	0.061
	$\angle\phi_a$	deg	−79.718	−52.956	−96.690	109.516	−57.187	−11.744	−139.004	10.942
	$\|U_b\|$	kV	59.642	0.203	3.109	1.905	0.150	0.765	0.336	0.014
	$\angle\Theta_b$	deg	−10.811	145.783	89.966	73.082	159.282	−174.214	173.811	−30.160
	$\|I_b\|$	A	556.354	1.717	77.622	19.332	0.822	2.885	0.687	0.123
	$\angle\phi_b$	deg	159.430	90.821	20.887	−9.964	76.562	103.961	100.552	102.694
	$\|U_c\|$	kV	59.736	0.119	2.814	1.925	0.097	0.793	0.344	0.003
	$\angle\Theta_c$	deg	−130.280	74.167	−148.930	−43.281	−66.388	−50.931	59.218	161.697
	$\|I_c\|$	A	558.635	1.243	79.480	21.055	0.634	3.188	0.727	0.137
	$\angle\phi_c$	deg	40.735	−160.066	143.284	−123.952	−162.139	−135.554	−23.451	−100.764
4	$\|U_a\|$	kV	61.116	0.130	0.772	0.326	0.025	0.116	0.056	0.004
	$\angle\Theta_a$	deg	110.029	−105.322	160.075	77.173	−91.595	−71.404	142.875	−52.193
	$\|I_a\|$	A	234.901	0.521	3.566	1.748	0.146	0.818	0.449	0.036
	$\angle\phi_a$	deg	−74.055	94.180	13.865	−58.780	142.389	166.160	23.541	−153.829
	$\|U_b\|$	kV	60.229	0.340	1.056	0.421	0.124	0.142	0.110	0.056
	$\angle\Theta_b$	deg	−10.985	−36.877	−88.132	−90.652	169.418	66.129	28.529	7.747
	$\|I_b\|$	A	254.092	3.003	4.154	2.227	0.066	0.775	0.398	0.092
	$\angle\phi_b$	deg	165.462	−120.628	144.224	168.822	81.240	−77.580	−95.080	71.632
	$\|U_c\|$	kV	60.362	0.448	1.052	0.143	0.131	0.097	0.102	0.059
	$\angle\Theta_c$	deg	−130.269	131.843	50.274	120.930	1.099	−167.016	−122.362	−175.438
	$\|I_c\|$	A	249.737	2.671	3.299	1.706	0.206	0.845	0.442	0.069
	$\angle\phi_c$	deg	44.300	50.139	−93.167	41.067	−52.129	39.592	150.828	−82.085

problem because most of the PQ monitoring devices do not give harmonic RMS and angle data. On a contrary, most of those devices measure only RMS values. One of the possible researches is finding equivalent phasor diagram on a certain interval in three-phase power networks. (3) A disadvantage of the proposed algorithm is its limitation solely to unloaded buses. There are special cases, i.e. conditions, under which HSE of unmonitored buses containing generation or consumption can be conducted. The stated disadvantage will be subject of continuation of this research. (4) One possible continuation of this research is analysis of different optimization tools with goal of having more accurate identification. (5) By introducing additional limitations in process of global matrix [$\mathbf{Y}(x, h)$] identification it is possible to asses exact transmission tower head geometry. This will be one of the future researches. (6) Transmission line model can be improved or already improved models can be used as shown in a reference [60]. One of the following future researches is comparative analysis of improved transmission line models and already existing models. (7) For implementation of this algorithm in real-time PS it is necessary to make a research of CT and VT influences on algorithm accuracy. This research can be experimentally conducted in power network with fewer number of nodes or using a simulation model. A simulation model represents deliberate input of errors in measurement process. Previously stated (measurements in real-time PS or simulation model) are going to be a completely new research.

7. Conclusions

HSE algorithm presented in this paper is based on matrix algebra and optimization methods.

Based on the accurate data about PS topology and partially know data it is possible to conduct satisfying HSE. Efficiency of the proposed HSE algorithm is demonstrated in case of 110 kV transmission network. Optimization GA has achieved an accuracy of 0.5% in identification of global admittance matrix. Maximum error of harmonic voltage estimation equals 1.129%, while an average error is 0.3%.

Table 3
Tabular presentation of voltage conditions estimation results of unmonitored PS part.

Bus	Label	Unit	h_1	h_3	h_5	h_7	h_9	h_{11}	h_{13}
5	$\|U_a\|$	kV	63.622	0.240	1.643	0.192	0.026	0.243	0.166
	$\angle\Theta_a$	deg	115.962	−76.219	−159.401	160.931	3.766	64.135	−70.590
	g	%	0.015	0.209	0.150	0.315	0.933	0.273	0.839
	$\|U_b\|$	kV	63.256	0.113	1.584	0.190	0.051	0.252	0.145
	$\angle\Theta_b$	deg	−4.155	134.346	−46.077	39.686	157.853	177.272	163.653
	g	%	0.001	0.870	0.050	0.218	0.557	0.100	0.448
	$\|U_c\|$	kV	63.422	0.138	1.776	0.193	0.031	0.259	0.146
	$\angle\Theta_c$	deg	−124.077	85.267	77.112	−73.383	−43.651	−58.559	58.031
	g	%	0.040	0.333	0.117	0.493	0.654	0.125	0.360
6	$\|U_a\|$	kV	61.977	0.242	1.364	1.206	0.078	0.577	0.327
	$\angle\Theta_a$	deg	113.180	−68.418	−56.617	−168.672	14.208	67.677	−67.316
	g	%	0.025	0.359	0.193	0.137	0.320	0.191	0.621
	$\|U_b\|$	kV	61.577	0.138	1.279	1.110	0.114	0.583	0.292
	$\angle\Theta_b$	deg	−6.930	142.349	70.642	70.563	159.151	−177.294	170.037
	g	%	0.017	0.448	0.082	0.111	0.019	0.048	0.300
	$\|U_c\|$	kV	61.744	0.123	1.129	1.136	0.072	0.604	0.296
	$\angle\Theta_c$	deg	−126.669	83.742	−175.363	−45.364	−58.002	−53.313	58.362
	g	%	0.028	0.981	0.264	0.044	0.689	0.120	0.246
7	$\|U_a\|$	kV	62.769	0.212	0.965	0.921	0.063	0.484	0.288
	$\angle\Theta_a$	deg	114.751	−70.537	−70.549	−170.543	12.528	66.858	−68.444
	g	%	0.020	0.396	0.196	0.143	0.391	0.214	0.645
	$\|U_b\|$	kV	62.369	0.102	0.833	0.835	0.101	0.490	0.253
	$\angle\Theta_b$	deg	−5.374	140.834	56.368	69.135	159.593	−178.877	168.182
	g	%	0.019	0.883	0.133	0.125	0.045	0.064	0.309
	$\|U_c\|$	kV	62.566	0.122	0.774	0.870	0.063	0.511	0.256
	$\angle\Theta_c$	deg	−125.225	89.445	164.826	−46.107	−51.651	−54.581	58.279
	g	%	0.024	**1.129**	0.239	0.060	0.844	0.113	0.292

Sensitivity analysis has shown several characteristics of proposed algorithm for harmonic estimation of unmonitored part of PS. (1) Geometric area of possible results ensures an existence of set of results having satisfying accuracy. (2) Harmonics of interest for global matrix [**Y**(x, h)] identification have the same trends, i.e. they have a high level of correlation. (3) Geometry obtained by optimization procedure does not represent actual nor equivalent transmission line tower head geometry. (4) Identification of global matrix [**Y**(x, h)] must be conducted only based on harmonics present in voltage and current waveforms of monitored PS buses. (5) For any default accuracy there is a set of results ensuring certain identification error of global matrix [**Y**(x, h)].

Based on necessary input data, it can be concluded that time of PS modeling is significantly shortened when using this algorithm. Modeling of each transmission line in the frequency domain is replaced with one equivalent model representing a certain set of transmission lines.

Comparison of error obtained by proposed HSE algorithm with literature shows certain major improvements. Important characteristic of this algorithm is uniform estimation error on all unmonitored buses. The unknown geometry that is estimated has contributed to improvement of HSE resluts.

Appendix A. Numerical simulation results

Tables 2 and 3 and scheme in Fig. 6 contain all necessary data needed to repeat HSE calculation. Fig. 6 shows configuration of the discussed 110 kV power network with its transmission lines lengths and transmission tower head type. Data about transmission tower head type are accurate values, however, those values the algorithm does not have on its disposal while identifying global conductance matrix. It is assumed that all 110 kV transmission lines have the same tower head type and that the entire geographical area of interest has same value of soil resistivity 100 Ωm.

The problem was simulated using following conditions: (1) The time simulation of 10 s after transient process. Time step, calculated using condition of upper frequency of interest 10 kHz and shortest transmission line, is $\triangle t$ = 24.41 μs. During the period of simulation, frequency of fundamental harmonic remains the same and is equal to 50 Hz. (2) Consumers connected to the buses 3 and 4 are elements of the simulation generating higher harmonics, asymmetry and flickers into the network. Buses 1 and 2 are electrical energy producing buses. (3) Calculation of harmonics is conducted for a time period of 200 ms [28,30,21].

As can be seen in Fig. 7 and in Table 2, the presence of 5th and 7th harmonic, besides the fundamental one, is obvious. Further analysis of only odd harmonics is made since system is in steady state.

References

[1] J.V. Milanovic, M. Bollen, N. Cukalevski, Guidelines for Monitoring Power Quality in Contemporary and Future Power Networks-Results From cigre/cired jwg c4. 112. CIGRE Sessions: 27/08/2014–30/08/2014, CIGRE, 2014, pp. 1–8, Available from: http://ltu.diva-portal.org/smash/get/diva2:1011477/FULLTEXT01.pdf [Online].
[2] J. Milanović, J. Meyer, R. Ball, W. Howe, R. Preece, M.H. Bollen, S. Elphick, N. Čukalevski, International industry practice on power-quality monitoring, IEEE Trans. Power Deliv. 29 (2) (2014) 934–941.
[3] J. Kilter, J. Meyer, S. Elphick, J.V. Milanovic, Guidelines for power quality monitoring-results from cigre/cired jwg c4. 112, in: 2014 IEEE 16th International Conference on Harmonics and Quality of Power (ICHQP), IEEE, 2014, pp. 703–707.
[4] A. Farzanehrafat, Power Quality State Estimation, 2014.
[5] A. Farzanehrafat, N.R. Watson, Review of power quality state estimation, in: Universities Power Engineering Conference (AUPEC), 2010 20th Australasian, IEEE, 2010, pp. 1–5.
[6] F.C. Schweppe, J. Wildes, Power system static-state estimation. Part I: Exact model, IEEE Trans. Power Appar. Syst. (1) (1970) 120–125.
[7] N. Watson, J. Arrillaga, Harmonics in large systems, Electr. Power Syst. Res. 66 (1) (2003) 15–29.
[8] Z.-P. Du, J. Arrillaga, N. Watson, Continuous harmonic state estimation of power systems, IEE Proc. – Gener. Transm. Distrib. 143 (4) (1996) 329–336, IET.
[9] K.P. Wong, N. Watson, J. Arrillaga, Sub-harmonic state estimation in power systems, in: Power Engineering Society Winter Meeting, 2000, IEEE, vol. 2, IEEE, 2000, pp. 1168–1173.
[10] C.F.M. Almeida, N. Kagan, Harmonic state estimation through optimal power quality, in: CIRED 21st International Conference on Electricity Distribution, Frankfurt, 2011, pp. 1220–1224.
[11] Z. Niancheng, L. Li, Z. Jizhong, An approach to harmonic state estimation of power system, J. Electromagn. Anal. Appl. 2009 (2009).

[12] S. Matair, N. Watson, K. Wong, V. Pham, J. Arrillaga, Harmonic state estimation: a method for remote harmonic assessment in a deregulated utility network, in: DRPT2000. International Conference on Electric Utility Deregulation and Restructuring and Power Technologies. Proceedings (Cat. No.00EX382), April, 2000, pp. 41–46, Available from: http://ieeexplore.ieee.org/lpdocs/epic03/wrapper.htm?arnumber=855636 [Online].
[13] C. Madtharad, S. Premrudeepreechacharn, N.R. Watson, Power system state estimation using singular value decomposition, Electr. Power Syst. Res. 67 (2) (2003) 99–107, Available from: http://www.sciencedirect.com/science/article/pii/S0378779603000804 [Online].
[14] N. Watson, J. Arrillaga, Z. Du, Modified symbolic observability for harmonic state estimation, IEE Proc. – Gener. Transm. Distrib. 147 (2) (2000) 105–111.
[15] H. Liao, Power system harmonic state estimation via sparsity maximization, in: Power Engineering Society General Meeting, 2006. IEEE, IEEE, 2006, p. 7.
[16] Z. Du, J. Arrillaga, N. Watson, S. Chen, Implementation of harmonic state estimation, 8th International Conference on Harmonics and Quality of Power. Proceedings (Cat. No.98EX227), vol. 1 (1998) 273–278.
[17] G. Heydt, Identification of harmonic sources by a state estimation technique, IEEE Trans. Power Deliv. 4 (1) (1989) 569–576.
[18] Z.-P. Du, J. Arrillaga, N. Watson, S. Chen, Identification of harmonic sources of power systems using state estimation, IEE Proc. – Gener. Transm. Distrib. 146 (1) (1999) 7–12, IET.
[19] J. Arrillaga, A. Medina, M.L.V. Lisboa, P. Sanchez, M.A. Cavia, The harmonic domain. a frame of reference for power system harmonic analysis, IEEE Trans. Power Syst. 10 (1) (1995) 433–440.
[20] A. Ketabi, S.A. Hosseini, A new method for optimal harmonic meter placement, Am. J. Appl. Sci. 5 (11) (2008) 1499–1505.
[21] A.G. Phadke, J.S. Thorp, Synchronized Phasor Measurements and Their Applications, Springer Science & Business Media, 2008.
[22] N. Shengsuo, L. Zhirui, S. Haifeng, G. Jun, Power system harmonic state estimation based on pmu and ridge estimation, in: 2010 China International Conference on Electricity Distribution (CICED), IEEE, 2010, pp. 1–6.
[23] A. Phadke, B. Pickett, M. Adamiak, M.M. Begovic, G. Benmouyal, J. Goossens, D.J. Hansen, M. Kezunovic, P. McLaren, G. Michel, Synchronized sampling and phasor measurements for relaying and control, IEEE Trans. Power Deliv. 9 (1) (1994) 442–452.
[24] T. Tan, S. Chen, S. Choi, An overview of power quality state estimation, 2005 International Power Engineering Conference (2005) 1–276, Available from: http://ieeexplore.ieee.org/lpdocs/epic03/wrapper.htm?arnumber=1627209 [Online].
[25] U. Arumugam, N.M. Nor, M.F. Abdullah, A brief review on advances of harmonic state estimation techniques in power systems, Int. J. Inf. Electron. Eng. 1 (3) (2011).
[26] A. Medina, J. Segundo-Ramirez, P. Ribeiro, W. Xu, K. Lian, G. Chang, V. Dinavahi, N. Watson, Harmonic analysis in frequency and time domain, IEEE Trans. Power Deliv. 28 (3) (2013) 1813–1821, Available from: http://ieeexplore.ieee.org/document/6514799/?arnumber=6514799 [Online].
[27] V. Becirovic, I. Pavic, S. Curevac, S. Hanjalic, B. Nikolic, N. Dozic, Voltage conditions estimation in frequency domain of power systems based on measuring power quality, in: 2015 5th International Youth Conference on Energy (IYCE), IEEE, 2015, pp. 1–8.
[28] International Electrotechnical Commission (IEC), IEC 61000-4-7: Electromagnetic Compatibility (EMC) Part 4–7: Testing and Measurement Techniques General Guide on Harmonics and Interharmonics Measurements and Instrumentation, for Power Supply Systems and Equipment Connected Thereto, Technical Norm, 2009.
[29] J. Barros, R.I. Diego, A new method for measurement of harmonic groups in power systems using wavelet analysis in the IEC standard framework, Electr. Power Syst. Res. 76 (4) (2006) 200–208.
[30] J.A.M. Phadke, A.G. Thorp, A new measurement technique for tracking voltage phasors, local system frequency, and rate of change of frequency, IEEE Trans. Power Appar. Syst. PAS-102 (1983), Available from: http://ieeexplore.ieee.org/document/036/4112 [Online].
[31] J. Arrillage, N.R. Watson, Computer Modelling of Electrical Power Systems, 2nd ed., J. Wiley and Sons, 2001.
[32] N. Tleis, Power Systems Modelling and Fault Analysis: Theory and Practice, Newnes, 2007.
[33] S. Sadović, Power System Analysis, University of Sarajevo, Faculty of Electrical Engineering in Sarajevo, 2004.
[34] A. Baggini, Handbook of Power Quality, John Wiley & Sons, 2008.
[35] C. Sankaran, Power Quality, CRC Press, 2001.
[36] C.D. Association, Earthing Practice, 119, CDA Publication, 1997.
[37] Z. Li, J. He, B. Zhang, Z. Yu, Influence of frequency characteristics of soil parameters on ground-return transmission line parameters, Electr. Power Syst. Res. 139 (2016) 127–132.
[38] A. Deri, G. Tevan, A. Semlyen, A. Castanheira, The complex ground return plane a simplified model for homogeneous and multi-layer earth return, IEEE Trans. Power Appar. Syst. (8) (1981) 3686–3693.
[39] M.E. El-Hawary, Electrical Power Systems: Design and Analysis, vol. 2, John Wiley & Sons, 1995.
[40] V. Perelmuter, Electrotechnical Systems: Simulation with Simulink and SimPowerSystems, har/cdr ed., ser TM. CRC Press, 2012.
[41] M.I. Alomoush, Exact pi-model of upfc-inserted transmission lines in power flow studies, IEEE Power Eng. Rev. 22 (12) (2002) 54–56.
[42] J. Roldan-Fernandez, F.M. Gonzalez-Longatt, J.L. Rueda, H. Verdejo, Modelling of transmission systems under unsymmetrical conditions and contingency analysis using digsilent powerfactory, in: PowerFactory Applications for Power System Analysis, Springer, 2014, pp. 27–59.
[43] G. Kron, Tensorial analysis of integrated transmission systems; Part IV. the interconnection of transmission systems [includes discussion], Power Appar. Syst. Part III. Trans. Am. Inst. Electr. Eng. 72 (2) (1953).
[44] J. Arrillaga, Power System Harmonic Analysis, John Wiley & Sons, 1997.
[45] F. Dorfler, F. Bullo, Kron reduction of graphs with applications to electrical networks, IEEE Trans. Circuits Syst. I: Regular Papers 60 (1) (2013) 150–163.
[46] J.A. Martinez-Velasco, Transient Analysis of Power Systems, vol. 1, IEEE PRESS, WILEY, Barcelona, 2015.
[47] H.W. Beaty, H. Mahrous, A.H. Seidman, Handbook of Electric Power Calculations, McGraw-Hill, New York, 2001.
[48] F.M. Uriarte, On kron's diakoptics, Electr. Power Syst. Res. 88 (2012) 146–150.
[49] W.A. Sutherland, Introduction to Metric and Topological Spaces, Oxford University Press, 1975.
[50] I.E. Commission, Iec 61000-4-30 Electromagnetic Compatibility (emc)-Part 4–30: Testing and Measurement Techniques-Power Quality Measurement Methods, 2008, Tech. Rep.
[51] D.P. Kroese, T. Taimre, Z.I. Botev, Handbook of Monte Carlo Methods, vol. 706, John Wiley & Sons, 2013.
[52] B. Iooss, P. Lemaître, A review on global sensitivity analysis methods, in: Uncertainty Management in Simulation-Optimization of Complex Systems, Springer, 2015, pp. 101–122.
[53] E. Din, 50160. Voltage Characteristics of Electricity Supplied by Public Distribution Networks, Last Review by, vol. 1, 2011.
[54] H.W. Dommel, Electromagnetic Transients Program: Reference Manual:(EMTP Theory Book), Bonneville Power Administration, 1986.
[55] B.M. Dehkordi, F.H. Fesharaki, A. Kiyoumarsi, Optimal measurement placement for static harmonic state estimation in the power systems based on genetic algorithm, J. Electr. Eng. Technol. 4 (2) (2009) 175–184.
[56] C. Madtharad, S. Premrudeepreechacharn, N.R. Watson, R. Saeng-Udom, An optimal measurement placement method for power system harmonic state estimation, IEEE Trans. Power Deliv. 20 (2) (2005) 1514–1521.
[57] M. Moghadasian, H. Mokhtari, A. Baladi, Power system harmonic state estimation using WLS and SVD; a practical approach, ICHQP 2010-14th International Conference on Harmonics and Quality of Power (2010).
[58] E.F. Arruda, N. Kagan, P. Ribeiro, Three-phase harmonic distortion state estimation algorithm based on evolutionary strategies, Electr. Power Syst. Res. 80 (9) (2010) 1024–1032.
[59] I.D. Melo, J.L. Pereira, A.M. Variz, P.A. Garcia, Harmonic state estimation for distribution networks using phasor measurement units, Electr. Power Syst. Res. 147 (2017) 133–144.
[60] A. De Conti, M.P.S. Emídio, Extension of a modal-domain transmission line model to include frequency-dependent ground parameters, Electr. Power Syst. Res. 138 (2016) 120–130.